Supplemental Data

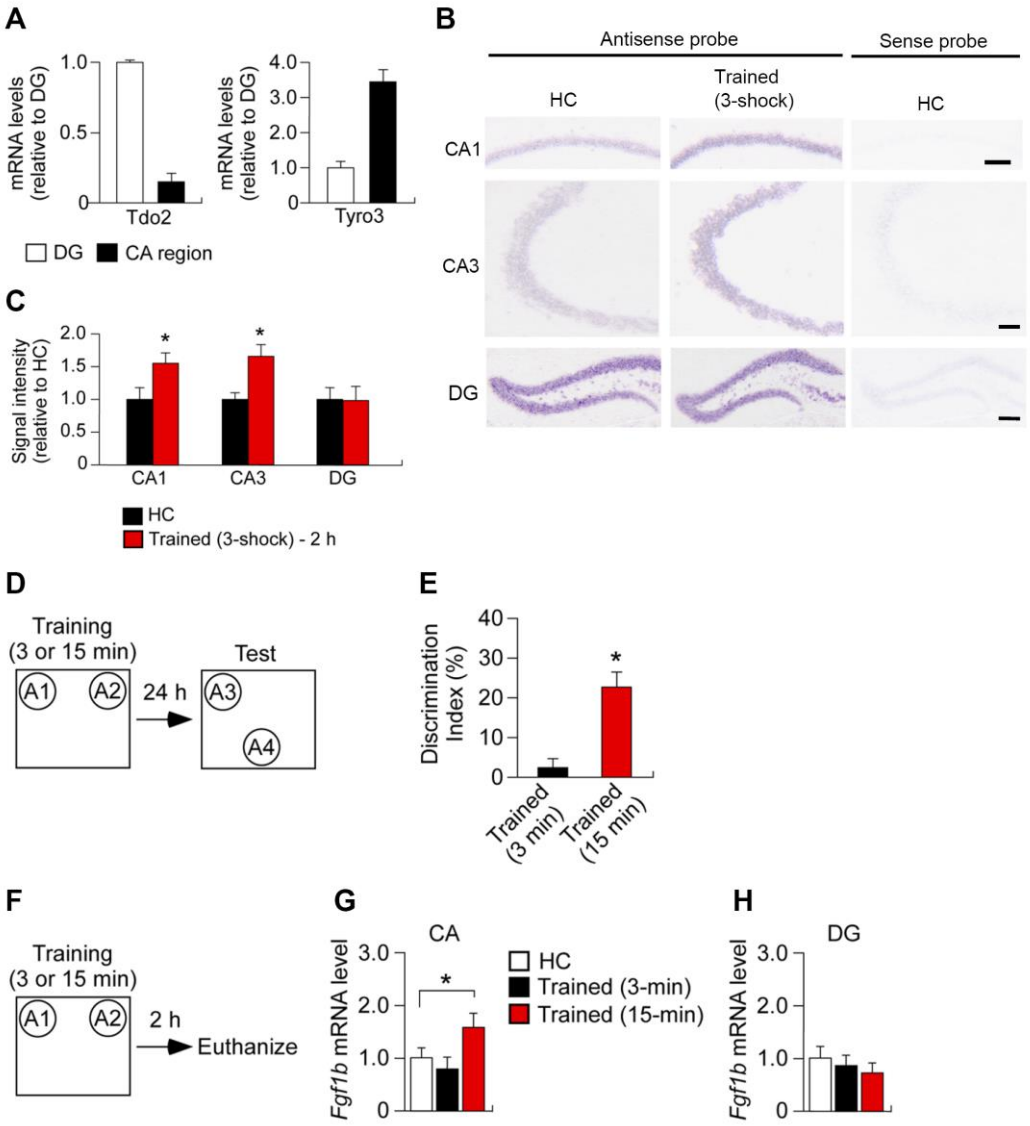

Figure S1. CA subregion-specific induction of *Fgf1b* mRNA following learning (related to Figure 1).
(A) Total RNA was isolated from the dentate gyrus (DG) and the cornu ammonis (CA) regions of the hippocampus. Specificity was confirmed by quantitative real-time PCR (Q-PCR) analysis of the DG-enriched gene *Tdo2* and the CA-enriched gene *Tyro3*. $n = 6$ mice/group.
(B and C) *In situ* hybridization. Digoxigenin-labeled *Fgf1* sense and anti-sense RNAs were hybridized with 20 µm thick coronal sections from trained mice 2 h after strong contextual fear conditioning (CFC, 3-shock) (middle panel) and sections from home cage (HC) control mice (left panel). No staining was detected using the sense RNA (right panel), demonstrating the specificity of the anti-sense probe. Scale bar, 100 µm. Quantitative analysis (C) revealed increased *Fgf1* mRNA expression in CA1 and CA3, but not in the DG, of mice subjected to three-shock CFC training. $n = 6$ mice/group. $^*p < 0.05$ versus the HC control (Student's *t*-test).
(D) Experimental design of the object location memory task. Mice were exposed to an environment with two identical objects for 3 or 15 min, followed by a retention test 24 h later in which one object was moved to a new location.
(E) Mice receiving 15 min of training showed a greater 24-h long-term memory compared with those receiving 3 min of training. $n = 10$ mice/group. $^*p < 0.05$ (Student's *t*-test).
(F) Experimental design of Q-PCR analysis. Mice were sacrificed 2 h after 3 or 15 min of training in the object location task.
(G and H) Q-PCR analysis of *Fgf1b* mRNA expression in CA (G) and DG (H) subregions of mice subjected to object location training (3 or 15 min). $n = 6$ mice/group. $^*p < 0.05$ (*post hoc* test).
Data are presented as mean ± SEM.

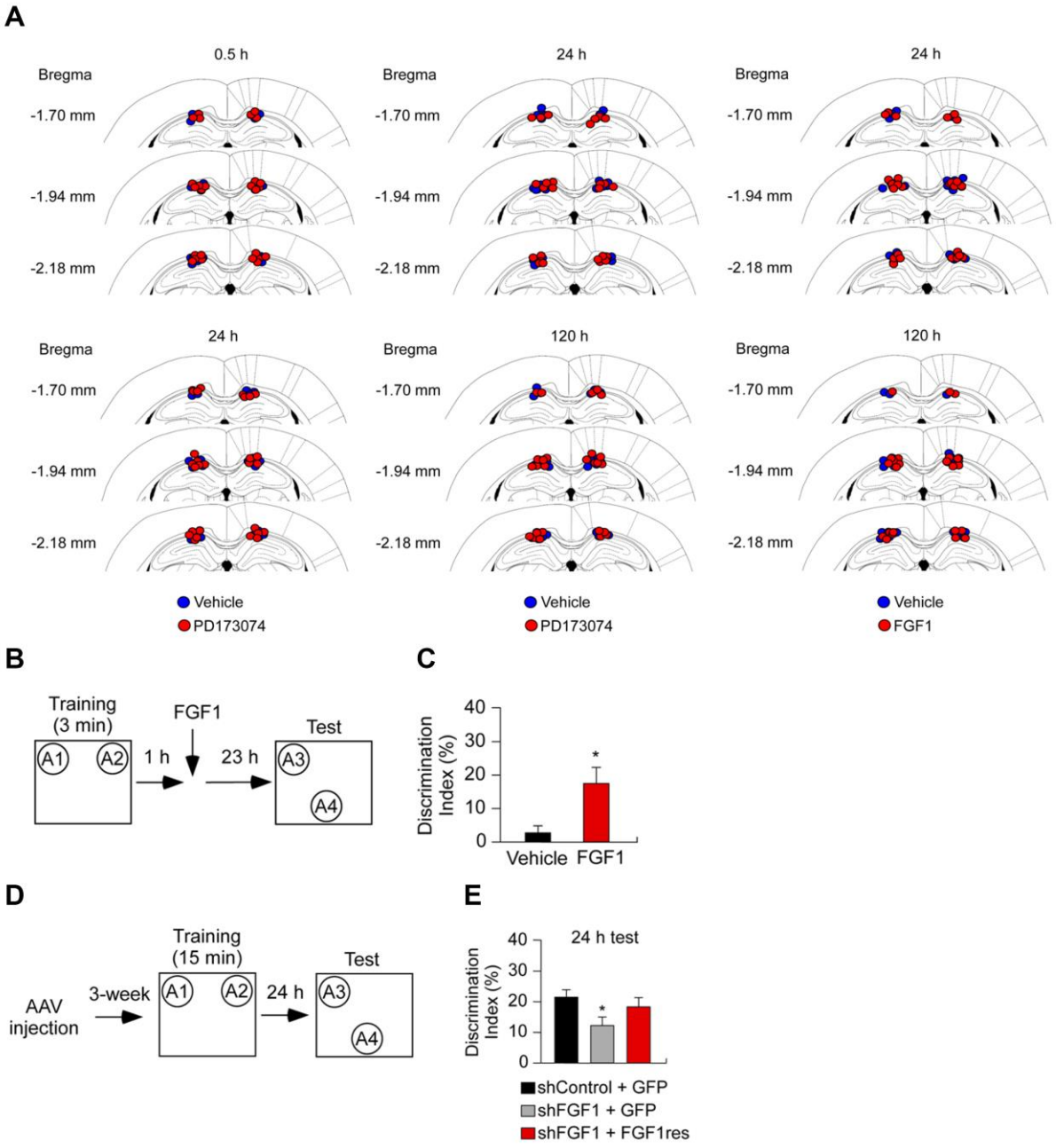

Figure S2. FGF1 is essential for memory formation (related to Figure 2).

(A) Left, locations of the cannula tips in mice infused with the FGF receptor inhibitor PD173074 (see corresponding Figure 2G). Middle, locations of the cannula tips in mice infused with PD173074 (corresponding to Figure 2I). Right, locations of the cannula tips in mice infused with recombinant FGF1 (corresponding to Figure 2K).

(B) Experimental design of the 3-min OLM task. Mice received 3 min of object location training and 1 h later were injected with recombinant FGF1 into bilateral hippocampus. Twenty-four hours after training, they were tested for OLM (24-h test).

(C) Mice injected with FGF1 showed increased OLM. n = 10–14 mice/group. *p < 0.05 versus vehicle (Student's t-test).

(D) Experimental design of the 15-min object location memory (OLM) task. Mice given AAV-shControl or AAV-shFGF1 together with AAV-GFP or AAV-FGF1res received 15 min of training in an environment with two identical objects and then a retention test 24 h later in which one object was moved to a new location.

(E) Mice injected with AAV-shFGF1 and AAV-GFP showed decreased OLM, whereas this reduction was not observed in mice injected with AAV-shFGF1 and AAV-FGF1res. n = 11–13 mice/group. *p < 0.05 versus mice given AAV-shControl and AAV-GFP (*post hoc* test).

Data are presented as mean ± SEM.

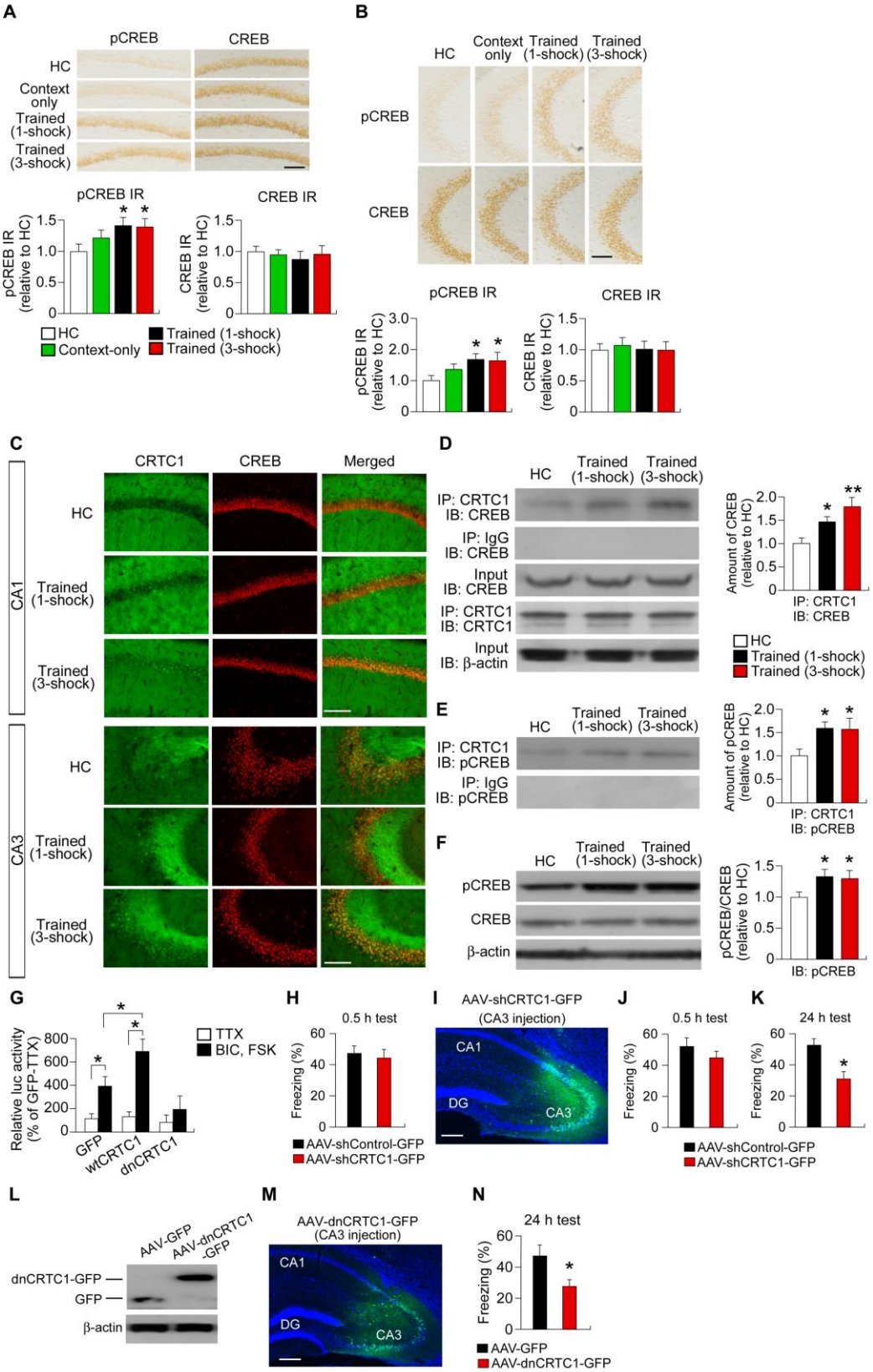

Figure S3. CRTC1 regulates memory formation (related to Figure 3).
(A and B) Immunostaining with an antibody against phosphorylated CREB (pCREB) revealed increased pCREB levels in the cornu ammonis (CA1) (A) and CA3 (B) of mice following contextual fear conditioning (CFC) compared with home cage (HC) control mice. Mice were euthanized 1 h after CFC training. There was no difference in pCREB levels between mice receiving one-shock (weak) and three-shock (strong) CFC training. n = 6 mice/group. *p < 0.05 versus HC controls (*post hoc* test). Scale bar, 100 μm.

(C) Representative images showing co-localization of endogenous CRTC1 (green) and CREB (red) in the CA1 and CA3 of mice subjected to CFC (one or three shocks). Scale bar, 100 μm.
(D) Co-immunoprecipitation showing the binding of CRTC1 to CREB in the CA subregion of mice subjected to CFC (one or three shocks). n = 6 mice/group. *$p < 0.05$, **$p < 0.01$ versus home cage (HC) controls (*post hoc* test).
(E) Co-immunoprecipitation showing binding of CRTC1 to pCREB-Ser133 in the CA subregion of mice subjected to CFC (one or three shocks). n = 6 mice/group. *$p < 0.05$ versus HC controls (*post hoc* test).
(F) Western blots showing pCREB levels in the nuclear fraction from the CA subregion of mice subjected to one- or three-shock CFC. n = 6 mice/group. *$p < 0.05$ versus HC controls (*post hoc* test).
(G) Bar graphs showing *Fgf1b* promoter-driven luciferase (luc) activity in primary hippocampal neuron cultures co-transfected with a luciferase reporter vector and either the GFP, wild-type CRTC1, or dominant-negative CRTC1 vector. Transfected neurons were treated with either tetrodotoxin (TTX) or bicuculline (BIC) and forskolin (FSK) for 6 h. n = 3 cultures/treatment. *$p < 0.05$ (*post hoc* test).
(H) Normal short-term contextual fear memory (CFM) in mice injected with AAV-shCRTC1-GFP into the CA1. n = 13 or 14 mice/group. *$p < 0.05$ (Student's *t*-test).
(I) AAV-shCRTC1-GFP microinjection into the CA3 induced robust GFP expression. Scale bar, 100 μm.
(J and K) Normal short-term CFM (I) and reduced long-term CFM (J) in mice injected with AAV-shCRTC1-GFP into the CA3. n = 13 or 14 mice/group. *$p < 0.05$ (Student's *t*-test).
(L) Western blot showing successful overexpression of dnCRTC1-GFP.
(M) AAV-shCRTC1-GFP microinjection into the CA3 induces robust GFP expression. Scale bar, 100 μm.
(N) Reduced CFM in mice injected with AAV-shCRTC1-GFP into the CA3. n = 13 or 14 mice/group. *$p < 0.05$ (Student's *t*-test).
Data are presented as mean ± SEM.

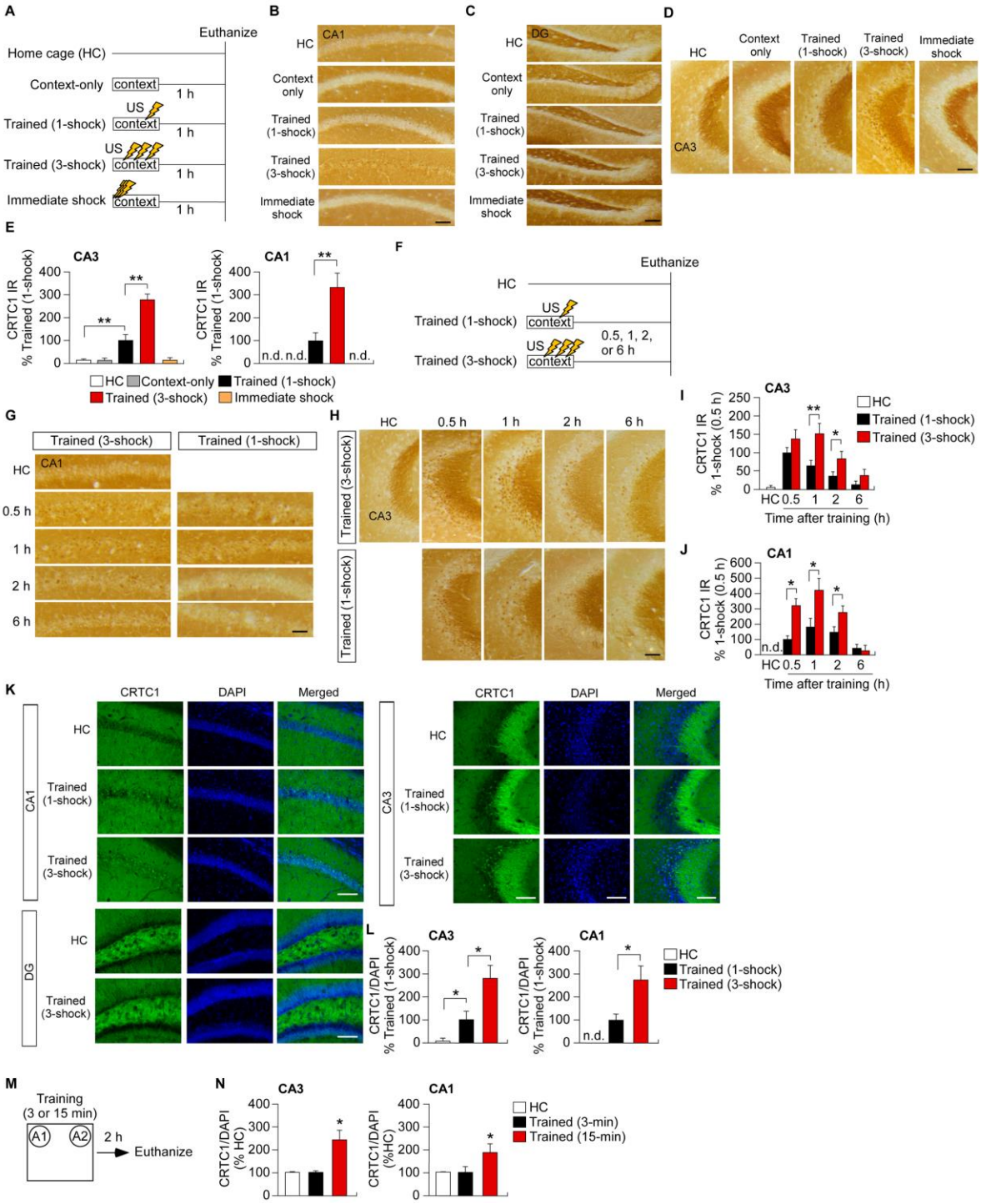

Figure S4. Learning-induced nuclear accumulation of CRTC1 correlates with strength of training (related to Figure 4).

(A) Experimental design for contextual fear memory. Mice were subjected to weak (one shock) or strong (three shocks) contextual fear conditioning (CFC) and sacrificed 1 h later for immunohistochemistry. Mice exposed to the context only (no foot shock) or to immediate shock (three foot shocks immediately after being placed in the chamber) and home cage (HC) mice were used as controls. US: unconditioned stimuli (foot shock).

(B–D) Representative images of CRTC1 immunoreactivity (IR) in the CA1 (B), dentate gyrus (DG) (C), and CA3 (D) of the hippocampus. Scale bar, 100 μm.

(E) Quantification of the number of CRTC1-positive cells in the CA3 and CA1. n.d.: not detected. n = 6 mice/group. $^{**}p < 0.01$ (*post hoc* test).

(F) Experimental design for CRTC1 immunohistochemistry (time-course experiment). HC: home cage. US: unconditioned stimuli (shock).

(G and H) Representative images of CRTC1 immunoreactivity (IR) in the CA1 (G) and CA3 (H). Scale bar, 100 μm.
(I and J) Percent CRTC1-positive cells in the CA3 (I) and CA1 (J). n.d.: not detected. $n = 6$ mice/group. *$p < 0.05$, **$p < 0.01$ (*post hoc* test).
(K) Representative images of CRTC1 immunofluorescence (green) in the CA1, CA3, and DG. DAPI (blue) used as a nuclear marker. Scale bar, 100 μm.
(L) Quantification of the nuclear CRTC1 signal in CA3 and CA1. $n = 6$ mice/group. *$p < 0.05$ (*post hoc* test).
Data are presented as mean ± SEM.
(M) Experimental design of the object location memory (OLM) task. Mice received 3 or 15 min of training in an environment with two identical objects and then were euthanized 2 h later.
(N) Quantification of the number of CRTC1-positive cells in the CA3 and CA1 following object location training. $n = 6–8$ mice/group. *$p < 0.05$ (*post hoc* test).

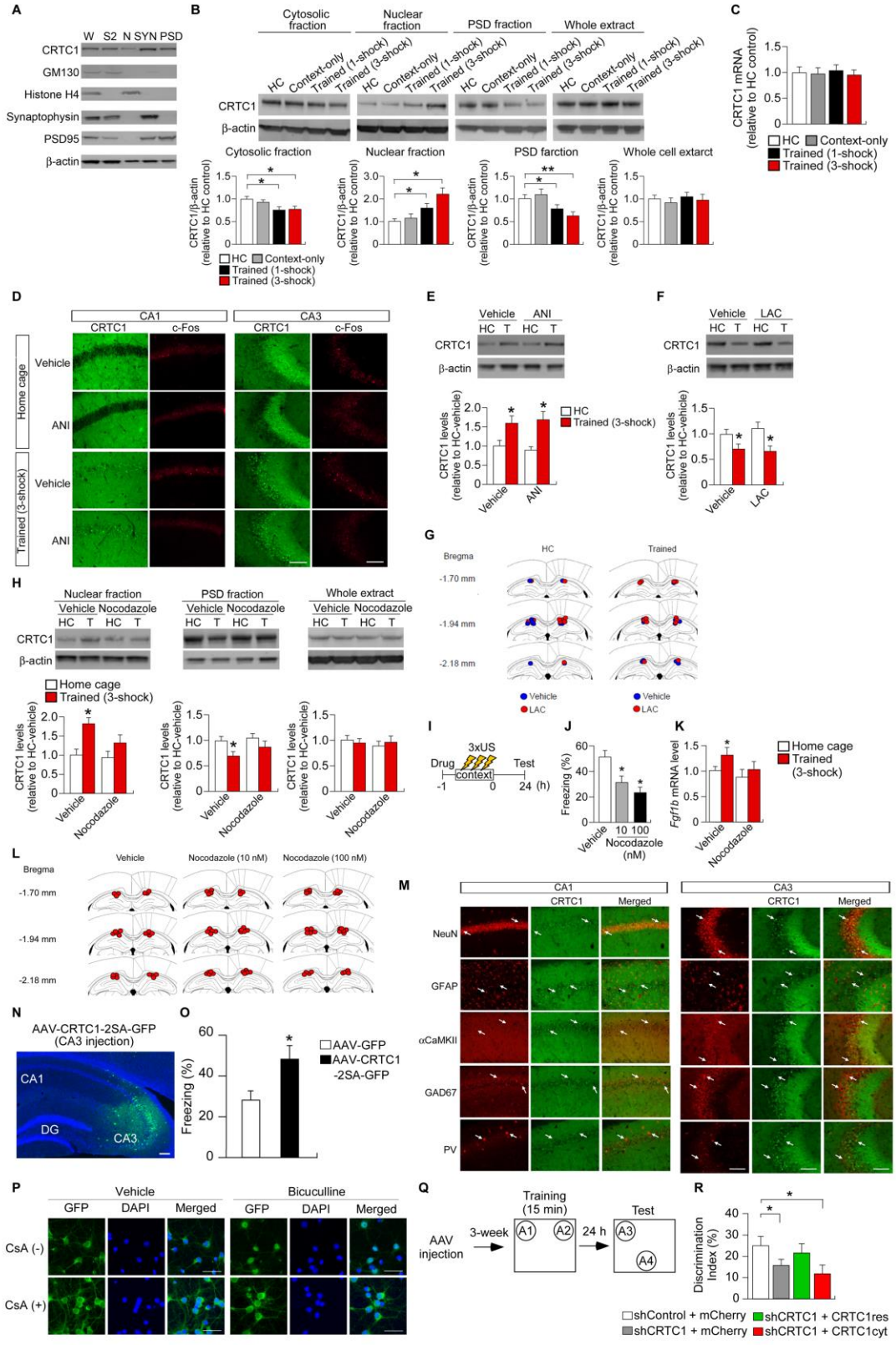

Figure S5. Nuclear translocation of CRTC1 is required for memory formation (related to Figure 4).
(A) The specificity of the PSD fraction was verified by immunoblotting for GM130 (Golgi marker), histone H4 (nuclear marker), synaptophysin (presynaptic marker), and PSD95 (postsynaptic marker). W, whole-cell extract; S2, cytosol and microsomes; N, nuclear fraction; SYN, synaptosomal fraction; PSD, PSD fraction.
(B) Western blot showing CRTC1 levels in the cytosolic, nuclear, and PSD fractions and in the whole-cell lysate from the CA region of mice subjected to context only or CFC training (one or three shocks) and home cage (HC) control mice. n = 6 mice/group. *$p < 0.05$, **$p < 0.01$ (*post hoc* test).

(C) Q-PCR analysis of *Crtc1* mRNA expression in the CA subregion of mice subjected to CFC (one or three shocks) or context only. n = 6 mice/group.
(D) Representative images of CRTC1 (green) and Fos (red) immunofluorescence 1 h after three-shock CFC in mice intraperitoneally injected with the protein synthesis inhibitor anisomycin (ANI) 30 min before training. Scale bar, 100 μm.
(E) Western blot showing CRTC1 levels in the CA nuclear fraction of ANI-treated mice 1 h after three-shock CFC. $n = 6$ mice/group. $^*p < 0.05$ vs. HC controls (*post hoc* test). T: trained.
(F) Western blot showing CRTC1 levels in the PSD fraction from the CA subregion of lactacystin (LAC)-treated mice 1 h after three-shock training. LAC was injected into the hippocampus 60 min before training. $n = 6$ mice/group. $^*p < 0.05$ vs. HC controls (*post hoc* test).
(G) Locations of the cannula tips in mice infused with lactacystin (LAC).
(H) Western blots showing nuclear, PSD, and whole-cell CRTC1 levels in the CA of mice pre-injected with nocodazole (100 nM) 1 h after three-shock CFC. Nocodazole was injected into the hippocampus 1 h before training. $^*p < 0.05$ vs. vehicle-treated HC group (*post hoc* test).
(I) Experimental design for CFM. Nocodazole was injected into the hippocampus 1 h before three-shock CFC and CFM assessed 24 h after training.
(J) CFM in mice injected with nocodazole (10 or 100 nM). $n = 12–14$ mice/group. $^*p < 0.05$ vs. vehicle-treated group (*post hoc* test).
(K) Q-PCR of *Fgf1b* mRNA expression in nocodazole-injected mice (100 nM) 2 h after three-shock CFC. n = 6 or 7 mice/group. $^*p < 0.05$ vs. vehicle-treated HC group (*post hoc* test).
(L) Locations of the cannula tips in mice infused with nocodazole.
(M) Representative images of the CA1 and CA3 of mice subjected to three-shock CFC showing colocalization of endogenous CRTC1 (green) with cell type-specific markers (red): mature neurons (NeuN), astrocytes (GFAP), excitatory neurons (αCaMKII), or interneurons (GAD67 and parvalbumin (PV). Scale bar, 100 μm.
(N) AAV-CRTC1-2SA-GFP microinjection into the CA3 induced robust GFP expression. Scale bar, 100 μm.
(O) Enhanced long-term object location memory (OLM) at 24 h in mice injected with AAV-CRTC1-2SA-GFP into the CA3. $n = 13$ or 14 mice/group. $^*p < 0.05$ (Student's *t*-test).
(P) Representative images of CRTC1 immunofluorescence (green) in hippocampal neuron cultures stimulated with bicuculline (BIC) or BIC and cyclosporin A (CsA). DAPI (blue) was used as a nuclear marker. Scale bar, 50 μm.
(Q) Experimental design for the OLM task. Mice injected with AAV-shControl or AAV-shCRTC1 together with AAV-mCherry, AAV-CRTC1res, or AAV-CRTC1cyt received 15 min of training in an environment with two identical objects. Mice were then subjected to a retention test 24 h later in which one object was moved to a new location.
(R) Mice injected with AAV-shCRTC1 and AAV-mCherry showed decreased OLM. The shCRTC1-mediated memory impairment was blocked by overexpression of CRTC1res but not by CRTC1cyt. $n = 13–15$ mice/group. $^*p < 0.05$ (*post hoc* test).
Data are presented as mean ± SEM.

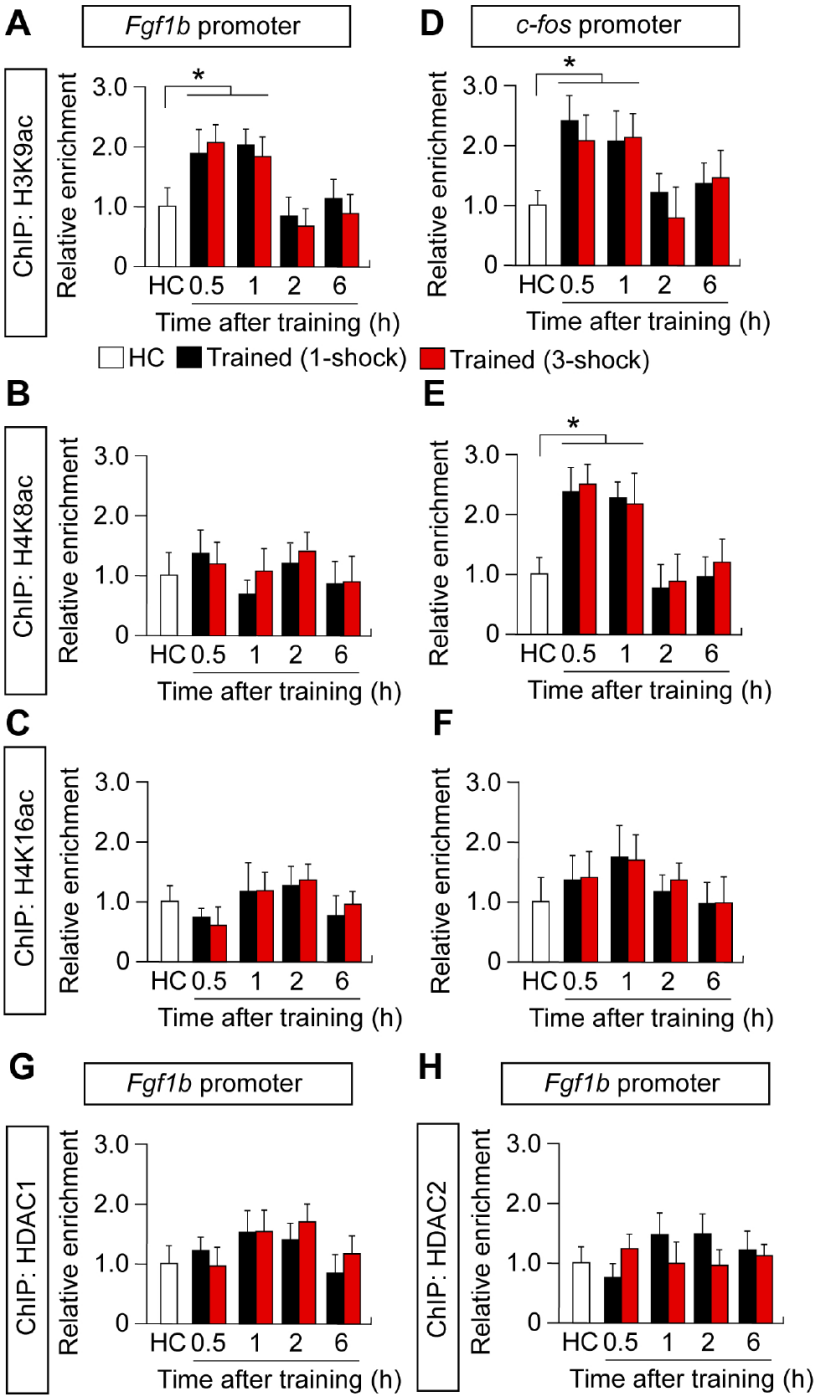

Figure S6. Histone acetylation at the *Fgf1b* and *c-fos* promoter following learning (related to Figure 5).
(A–C) Chromatin immunoprecipitation (ChIP) assay showing recruitment of H3K9ac, H4K8ac, and H4K16ac to the *Fgf1b* promoter 0.5 h, 1 h, 2 h, and 6 h after contextual fear training (CFC, one or three shocks). n = 6–10 samples/group. *$p < 0.05$ (*post hoc* test).
(D–F) ChIP assay showing the occupancy levels of H3K9ac, H4K8ac, and H4K16ac on the *c-fos* promoter 0.5, 1, 2, or 6 h after CFC training (one or three shocks). n = 6–10 samples/group. *$p < 0.05$ (*post hoc* test).
(G and H) ChIP assay showing recruitment of HDAC1 (G) and HDAC2 (H) to the *Fgf1b* promoter 0.5, 1, 2, or 6 h after CFC training (one or three shocks). n = 6–10 samples/group.
Data are presented as mean ± SEM.

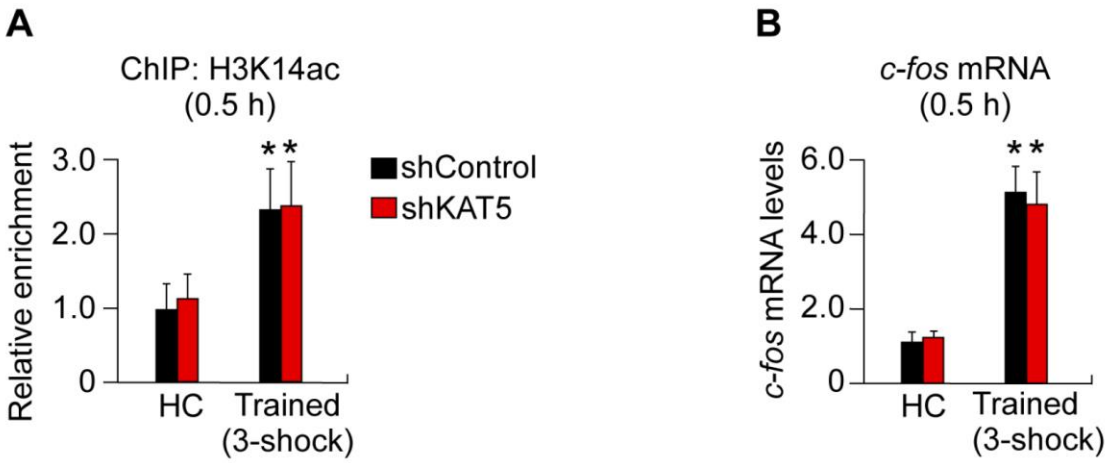

Figure S7. Effect of KAT5 knockdown on histone acetylation at the *c-fos* promoter and *c-fos* mRNA induction (related to Figure 7).

(A) Chromatin immunoprecipitation (ChIP) assay showing H3K14ac occupancy on the *c-fos* promoter 0.5 h after contextual fear training (three shocks) compared with home cage (HC) controls. n = 5–8 samples/group. *p < 0.05 versus HC controls (*post hoc* test).

(B) Q-PCR analysis of *c-fos* mRNA expression in the CA subregion of mice injected with AAV-shKAT5 0.5 h after CFC (three shocks) compared with HC controls. n = 6 mice/group. *p < 0.05 versus HC controls (*post hoc* test).

Data are presented as mean ± SEM.

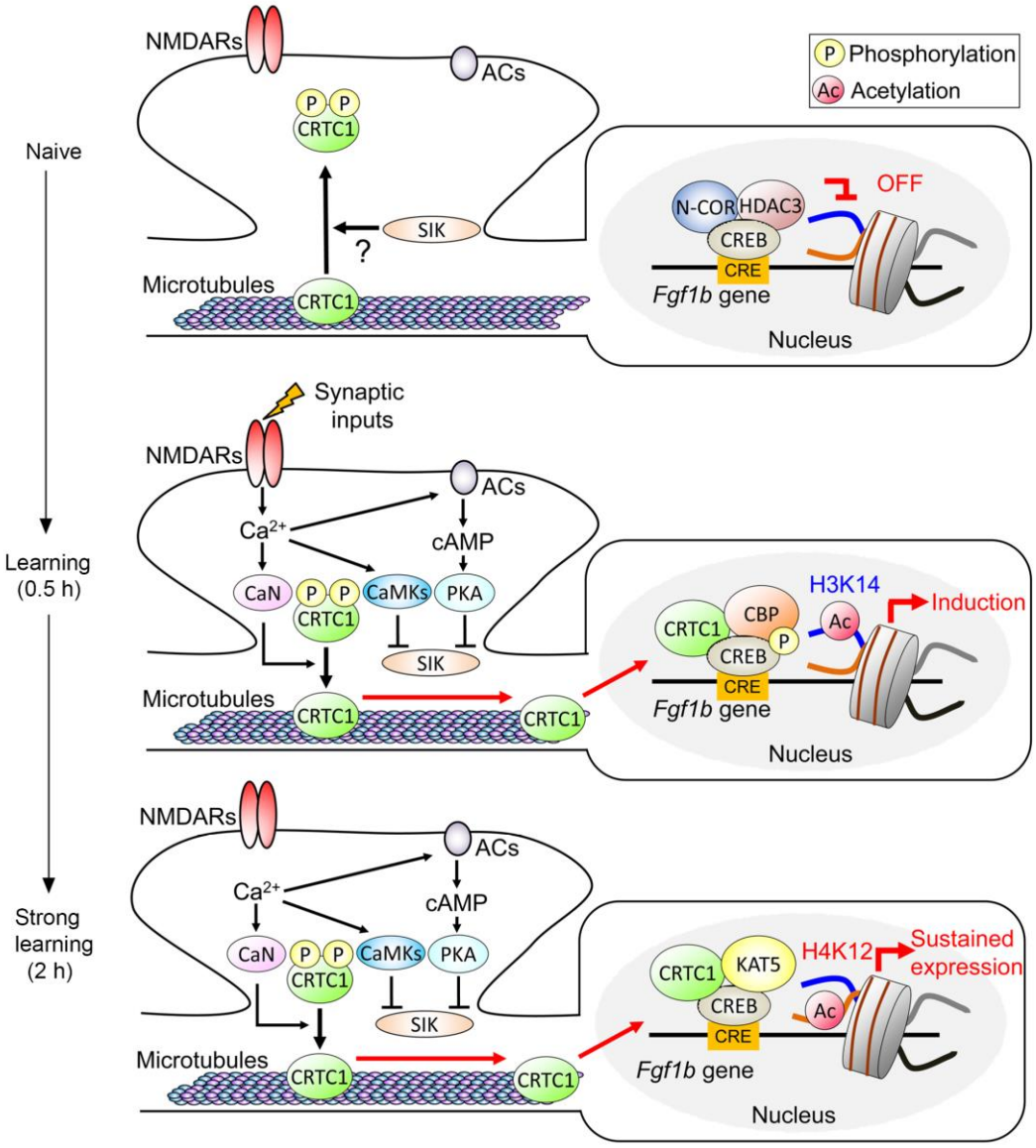

Figure S8. Proposed model how CRTC1 controls *Fgf1b* transcription and enhances memory (related to Discussion).

Under basal conditions, CRTC1 is phosphorylated and anchored to the synapses and dendrites. In the nucleus, HDAC3–N-CoR complex represses *Fgf1b* transcription. Upon learning, Ca^{2+} and cAMP signals potentiate CRTC1 dephosphorylation via inhibition of salt-inducible kinases (SIKs) and activation of calcineurin (CaN), respectively. Dephosphorylated CRTC1 translocates to the nucleus, where it binds to phosphorylated CREB (pCREB) and histone acetyltransferases (CBP) and enhances *Fgf1b* gene transcriptional activity by increasing the acetylation of H3K14 on its promoter. Strong training (*e.g.*, three foot-shock contextual fear conditioning) maintains nuclear localization of CRTC1 and upregulates *Fgf1b* transcription independently of pCREB even 2 h after learning by enhancing H4K12 acetylation via KAT5 recruitment to its promoter region. Learning-induced KAT5 recruitment acetylates H4K12 on the *Fgf1b* promoter, thereby enhancing synaptic plasticity and memory formation. For details, see Discussion.

Table S1. List of all primer sequences used in real time PCR, ChIP assay, and cloning.

Table S2. List of all primary antibodies used in this study.

Supplemental Experimental Procedures

Contextual fear conditioning

Contextual fear conditioning (CFC) was performed as described previously (Shumyatsky et al., 2005). Mice were singly housed for at least 7 days prior the behavioral test. For single foot-shock CFC (weak training), each mouse was placed in the conditioning chamber (Med Associates) for 238 s before the onset of a 2-s foot-shock [0.75 mA, unconditioned stimulus (US)). After an additional 60 s in the chamber, the mouse was returned to its home cage. Twenty-four hours after training, the mouse was placed back in the chamber, and the time spent freezing was assessed for 3 min using FreezeView software (Coulbourn Instruments). For three foot-shock CFC (strong training), each mouse was placed in the conditioning chamber for 300 s. The mouse was allowed to explore the chamber from 118 s before the first of three foot-shocks (0.75 mA, 2 s) delivered at 58-s intervals. After the last US, the mouse remained in the box for 60 s before being returned to its home cage. Assessment was performed as described above 24 h later.

Object location memory task

This task was performed as reported previously (McQuown et al., 2011; Vogel-Ciernia et al., 2013). Mice were singly housed for at least 7 days prior the behavioral test. Before training, mice were handled 2 min/day for 5 consecutive days and habituated to the experimental apparatus 5 min/day for 4 days in the absence of objects. In the training trial, mice were placed in the experimental apparatus with two identical objects (A1 and A2) and allowed to explore these objects for 3 min (weak training) or 15 min (strong training). During the 24-h retention test, mice were placed into the experimental apparatus for 5 min. One copy of the familiar object (A3) was placed in the same location as during the training trial and one copy of the familiar object (A4) was placed in a different location from the training trial. All training and testing trials were videotaped and analyzed using ANY Maze software (Stoelting). The relative exploration time around each object (t_{An}) was recorded and expressed by a discrimination index ($DI = (t_{A4} - t_{A3}) / (t_{A4} + t_{A3}) \times 100\%$).

Primary hippocampal neuron cultures

Primary hippocampal neurons were prepared from embryonic day 17 (E17) mouse embryos. After the removal of the brains, the hippocampi were dissected and dissociated, and the tissue pieces incubated in 2.5% trypsin (Life Technologies) for 20 min at 37°C. Dissociated cells were then incubated with a trypsin inhibitor (Worthington) and resuspended in DMEM containing 10% FBS. Viable cells, as indicated by trypan blue exclusion, were seeded on poly-D-lysine-coated 24-well dishes. Four hours after plating, the medium was replaced with Neurobasal medium (Life Technologies) containing 1% B27 supplement (Life Technologies) and 50 μg/ml streptomycin. The cultures were maintained at 37°C in a humidified 5% CO_2 atmosphere. On day 2 *in vitro* (2 DIV), hippocampal neurons were treated with 2 μM 1-β-D-arabinofuranosylcytosine (AraC, Sigma) to reduce the number of proliferating non-neuronal cells. Prior to measuring FGF family mRNA levels by Q-PCR (Figure 1A), primary neurons at 10 DIV were pretreated with MK-801 or vehicle for 1 h and then treated with bicuculline (50 μM) for 2 h. For luciferase assays (Figure S3G), primary neurons at 4 DIV were cotransfected with pGL3-*Fgf1b* promoter-driven luciferase plasmids together with expression plasmids encoding wild-type CRTC1, dominant negative CRTC1, or GFP. The primer sequences for PCR amplification and mutagenesis are shown in Table S1. Forty-eight hours after transfection, hippocampal neurons were treated with TTX (1 μM) or bicuculline (50 μM) and forskolin (20 μM) for 6 h. For CRTC1 imaging (Figure S5P), primary neurons at 10 DIV were treated with bicuculline (30 μM) in the presence or absence of cyclosporin A (1 μM) for 2 h. For GFP imaging following KCl and forskolin stimulation (Figures 4A), hippocampal neurons at 6 DIV were transfected with plasmids expressing wild-type CRTC1-GFP, CRTC1-S151A-GFP, CRTC1-S167A-GFP, or CRTC1-2SA-GFP (primer sequences for PCR amplification and mutagenesis are shown in Table S1) using Lipofectamine 2000 reagent (Life Technologies) according to the manufacturer's protocol. After 16 h, transfected neurons were

incubated in KCl (50 mM) and forskolin (20 μM) or vehicle for 1 h followed by recovery (washout) for 1 h. For GFP imaging following bicuculline stimulation (Figures 4G), hippocampal neurons at 6 DIV were transfected with plasmids expressing wild-type CRTC1-GFP or CRTC1cyt-GFP (primer sequences for PCR amplification and mutagenesis shown in Table S1) using Lipofectamine 2000 reagent. After 16 h, transfected neurons were incubated in bicuculline (50 μM) or vehicle for 2 h.

RNA extraction, cDNA synthesis, and Real-time PCR

Quantitative real-time PCR (Q-PCR) analysis was performed as previously reported (Uchida et al., 2011b). The dissection of the DG and CA regions was performed as previously reported (Hagihara et al., 2009; Kerimoglu et al., 2013). Total RNA from hippocampal neuron cultures and dissected tissues was extracted using TRIzol Reagent (Life Technologies) and treated with DNase (DNA free; Applied Biosystems). The RNA quality was verified by the A_{260}/A_{280} ratio, which was 1.91–2.03 for all RNA preparations. One microgram of total RNA was reverse transcribed to cDNA using the TaqMan Gold RT-PCR kit (Life Technologies). The cDNA was stored at −80 °C until use. Real-time PCR was performed using the Applied Biosystems 7900HT Fast Real-Time PCR System with SYBR green PCR Master Mix (Applied Biosystems) according to the manufacturer's protocol. PCR conditions were 10 min at 95 °C, followed by 40 cycles at 95 °C for 15 s and 60 °C for 30 s. Primer sequences are shown in Table S1. Amplification curves were visually inspected to set a suitable baseline range and threshold level. The relative quantification method was employed according to the manufacturer's protocol in which all target mRNA expression levels were normalized to *Gapdh* expression and verified by normalization to *β-actin*. All measurements were performed in triplicate.

Immunocytochemistry of primary hippocampal neurons

Neurons treated as indicated were washed with 1X PBS, fixed using 4% paraformaldehyde in PBS, blocked in PBS containing 5% BSA and 0.3% Triton X-100, and then incubated in primary antibodies against GFP, MAP2 (a neuronal marker), and/or CRTC1 at 4°C overnight. After washing in PBS, neurons were incubated in Alexa Fluor 488-conjugated anti-rabbit IgG and Alexa Fluor 568-conjugated anti-mouse IgG, washed, counterstained with DAPI, and mounted using mounting medium. Images were acquired using a Zeiss Axio Observer microscope and/or LSM 510 META laser confocal microscope (Zeiss). The images were analyzed using AxioVision software (Zeiss). The primary antibodies used are described in Table S2.

Luciferase reporter assay

For the reporter construct, a 1801-bp DNA fragment of the *Fgf1b* promoter containing the CRE1 site and a major transcription start site (see Figure 3A) was amplified by PCR using specific primers (Table S1). The resulting DNA fragment was cloned into the pGL3-basic luciferase reporter vector (Promega). This construct was verified by DNA sequencing. A pCMV-β-galactosidase vector (0.1 μg/well) was also cotransfected as a control for transfection efficiency. In all cases, the total amount of transfected plasmid DNA per well matched that of the empty plasmid. Forty-eight hours after transfection, the luciferase and β-galactosidase activities were measured using a luciferase assay system (Promega) and a β-galactosidase assay system (Promega). Luciferase activity was normalized to β-galactosidase activity. All reporter assays were performed in triplicate for at least three independent experiments.

***In situ* hybridization**

In situ hybridization was performed as previously reported (Schaeren-Wiemers and Gerfin-Moser, 1993; Shumyatsky et al., 2005). To clone mouse *Fgf1* cDNA, 1 μg of total RNA isolated from the mouse hippocampus was reverse transcribed using oligo-dT 16 (Applied Biosystems), and cDNA was amplified by PCR using specific primers (Table S1). The resulting PCR product was cloned into the pGEM-T Easy vector (Promega). The construct was validated by restriction site analysis and sequencing. The *Fgf1* antisense riboprobe was generated from the plasmid linearized with *Bam*HI and transcribed with SP6 RNA polymerase. The sense riboprobe was synthesized after linearization with *Hin*dIII and transcription with T7 RNA polymerase. The riboprobes were transcribed in the presence of DIG-UTP (Roche) for DIG labeling. Coronal sections of fresh-frozen mouse brains were prepared at 20 μm thickness using a cryostat (Leica) and hybridized according to a published protocol with modifications (Schaeren-Wiemers and Gerfin-Moser, 1993). Briefly, the sections were

fixed with 4% paraformaldehyde in 0.1 M PBS, pH 7.4, for 10 min, rinsed in PBS treated with diethylpyrocarbonate (DEPC), and treated with acetic anhydride in 0.1 M triethanolamine/distilled water for 10 min at room temperature. Next, the sections were washed in PBS-DEPC solution and incubated in prehybridization buffer (50% formamide, 5X SSC, 5X Denhardt's solution, 250 μg/ml *Escherichia coli* tRNA, and 500 μg/ml herring sperm DNA) for 1 h at room temperature. Hybridization was performed overnight at 45°C in prehybridization buffer. After hybridization, the sections were washed in 5X SSC at 45°C. After high-stringency washing [three times in 0.2X SSC at 45°C followed by 0.2X SSC at room temperature and B1 (0.1 M Tris-HCl, pH 7.5, 0.15 M NaCl)], the sections were processed for immunological detection of the DIG-labeled probes using an alkaline phosphatase (AP)-conjugated anti-DIG antibody (Roche) overnight at 4°C. The AP reaction was visualized using NBT/BCIP (Promega). Stained sections were then mounted on slides and coverslipped. Quantification of DIG-positive cells in the dorsal hippocampus (CA1, CA3, and dentate gyrus) was conducted using a computerized image analysis system (Image Pro 7.0). Immunoreactive cells were counted bilaterally using a fixed-sample window across at least five sections by an experimenter who was blind to the treatment condition.

Subcellular fractionation

Subcellular fractionation was performed as previously reported (Milnerwood et al., 2010; Pacchioni et al., 2009). For whole-tissue lysates, freshly dissected tissues were homogenized in ice-cold RIPA buffer (50 mM Tris, pH 8.0, 1% Triton X-100, 0.1% SDS, 150 mM NaCl) containing protease and phosphatase inhibitor cocktail tablets (Roche Applied Science). Nuclear, S2, synaptosomal, and PSD fractions were isolated according to an adopted protocol (Milnerwood et al., 2010; Pacchioni et al., 2009) with minor modifications. In brief, the tissues were homogenized in cold buffer (0.32 M sucrose, 50 mM NaF, and 10 mM HEPES, pH 7.4). The homogenates were centrifuged at 1000 × *g* for 10 min to yield the nuclear enriched pellet and again at 1000 × *g* for 10 min to yield the S1 fraction. To obtain the S2 fraction, the S1 fraction was centrifuged at 12,000 × *g* for 20 min at 4°C, and the supernatants (microsomes and cytosol) were collected. To obtain the synaptosomal fraction, the S1 fraction was filtered using a nitrocellulose filter (5 μm, Millipore) and centrifuged at 1000 × *g* for 20 min. The synaptosomal pellet was rinsed twice in buffer (4 mM HEPES, 1 mM EDTA, pH 7.4) and centrifuged for 20 min at 12,000 × *g*. The resulting pellet was incubated for 15 min in buffer (20 mM HEPES, 100 mM NaCl, 0.5% Triton X-100, pH 7.2) and then centrifuged at 12,000 × *g* for 20 min. The supernatant (Triton-soluble NP fraction) containing non-PSD membranes was retained. The pellet was resuspended in buffer (20 mM HEPES, 0.15 mM NaCl, 1% Triton X-100, 1% deoxycholic acid, and 1% SDS, pH 7.5) for 1 h and then centrifuged at 10,000 × *g* for 15 min. The supernatant contained the PSD (or Triton-insoluble) fraction. The nuclear fraction was isolated as previously reported (Milnerwood et al., 2010). The nuclear-enriched pellets were solubilized in 200 μl of nuclear buffer (10 mM HEPES/KOH, 10 mM KCl, 10 mM EDTA, 1.5 mM $MgCl_2$, 0.2% BSA, 1 mM DTT, 0.4% NP40, and protease and phosphatase inhibitors) followed by gentle rotating (15 min, 4°C). The samples were centrifuged at 15,000 × *g* for 10 min at 4°C, and the pellets retained as the crude nuclear fraction. The pellets were washed with 500 μl of nuclear buffer, followed by centrifugation at 15,000 × *g* for 10 min at 4°C. The supernatant was discarded and the pellets solubilized in buffer (20 mM HEPES/KOH, 400 mM NaCl, 1 mM EDTA, 10% glycerol, 1 mM DTT, protease and phosphatase inhibitors) followed by gentle vortexing. The samples were gently rotated for 2 h at 4°C, gently vortexed (3 s), and centrifuged at 15,000 × *g* for 10 min at 4°C to yield the nuclear extract (supernatant) and the nuclear envelope (pellet). The protein concentrations were measured using a BCA protein assay (Thermo Scientific).

Western blotting

Western blotting was performed as previously reported (Uchida et al., 2011a; Uchida et al., 2011b). Equal amounts of protein were separated on 12% Bis-Tris gels (Life Technologies), and transblotted onto polyvinylidene difluoride membranes (GE Healthcare Bio-Sciences). After blocking with 5% skim milk or 5% BSA, the membranes were incubated with primary antibodies against target proteins (Table S2). After incubation with appropriate horseradish peroxidase-conjugated secondary antibodies (HRP-linked anti-mouse IgG, HRP-linked anti-rabbit IgG, or HRP-linked anti-goat IgG antibody), the blots were developed using the ECL-Plus detection Kit (GE Healthcare Bio-Sciences or Thermo Scientific). When phospho-specific antibodies were used, all buffers included sodium fluoride (50 mM). Densitometric analysis was performed using ImageQuant software (GE Healthcare) after scanning (Typhoon, GE Healthcare).

3′3′-Diaminobenzidine (DAB) immunostaining

Mice were deeply anesthetized by intraperitoneal injection of Avertin (250 mg/kg body weight) and transcardially perfused with 4% paraformaldehyde and 1 mM sodium fluoride (NaF) in 0.1 M phosphate buffer (pH 7.4). The brains were post-fixed for 3 days, and 30-µm sections were prepared using a cryostat. For CRTC1 immunolabeling, the sections were first incubated in 3% hydrogen peroxide in 1X PBS for 1 h to quench endogenous peroxidase activity, then for 30 min in 10 mM sodium citrate buffer (pH 8.5) for antigen retrieval. Sections were blocked at room temperature in 1X PBS containing 2% skim milk and 0.3% Triton X-100 and incubated in the primary antibody against CRTC1 in 1% goat serum solution overnight at 4°C, followed by biotin-conjugated anti-rabbit IgG antibody (Vector Laboratories) diluted in 1% goat serum for 2 h at room temperature. After rinsing, the sections were treated with avidin and biotinylated horseradish peroxidase macromolecular complex reagent (VECTASTAIN Elite ABC kit, Vector Laboratories) for 1 h in the dark at room temperature prior to staining with DAB (ACRO Organics). All labeled sections were mounted on slides and coverslipped using Permount. For CREB and pCREB immunolabeling, the sections were incubated in 3% hydrogen peroxide in 1X PBS for 1 h, followed by incubation in blocking solution containing 1 mM NaF, 1% goat serum albumin, 1 mg/ml BSA, and 0.05% Triton X-100 for 3 h. Sections were then incubated in a primary antibody against CREB or pCREB in blocking solution overnight. After washing, sections were incubated for 2 h at room temperature in biotin-conjugated anti-rabbit IgG antibody diluted in blocking solution, rinsed, and treated with the avidin and biotinylated horseradish peroxidase macromolecular complex reagent for 1 h in the dark at room temperature prior to staining with DAB. All labeled sections were mounted on slides and coverslipped using Permount. The number of CRTC1-positive neurons was measured in the dorsal hippocampus (AP: −1.46 and −1.82 mm Bregma;(Franklin and Paxinos, 2008). Quantification of pCREB- or CREB-positive cells in the dorsal hippocampus was conducted using a computerized image analysis system (Image Pro 7.0). Immunoreactive neurons were counted bilaterally using a fixed sample window across at least five sections by an experimenter blind to the treatment condition. The primary antibodies are described in Table S2.

Immunofluorescence

Mice were deeply anesthetized by intraperitoneal injection of Avertin (250 mg/kg body weight) and transcardially perfused with 4% paraformaldehyde and 1 mM sodium fluoride (NaF) in 0.1 M phosphate buffer (pH 7.4). The brains were post-fixed for 3 days, and 30-µm sections were prepared using a cryostat. For CRTC1 immunofluorescence, sections were heated in antigen retrieval buffer and then incubated in blocking solution containing 5% bovine serum albumin and 0.3% Triton X-100 for 1 h at room temperature. The sections were then treated for 48 h at 4°C with the primary antibody against CRTC1 alone or together with a primary antibody against NeuN, GFAP, αCaMKII, GAD67, parvalbumin, or CREB. The secondary antibodies used were biotin-conjugated anti-rabbit IgG (Jackson ImmunoResearch) and Alexa Fluor 568-conjugated anti-mouse IgG (Life Technologies). After rinsing, sections were incubated in fluorescein-avidin D (Vector Laboratories). For c-Fos, GFP, and mCherry immunofluorescence, sections were treated overnight at 4°C with the primary antibody. After incubating the section with appropriate secondary antibody, images were acquired using a Zeiss Axio Observer microscope and/or LSM 510 META laser confocal microscope (Zeiss). Images were analyzed using AxioVision software (Zeiss). The primary antibodies used are described in Table S2.

Electrophysiology

Transverse hippocampal slices (400 µm) were prepared from adult (8-9 week old) C57BL/6J mice. Slices containing the dorsal part of the hippocampus were continuously superfused (2–3 ml/min) with artificial CSF (ACSF) containing (in mM) 125 NaCl, 2.5 KCl, 2 $CaCl_2$, 2 $MgSO_4$, 1.25 NaH_2PO_4, 26 $NaHCO_3$, and 10 glucose (~295 Osm), with 95% O_2/5% CO_2 at 31–32°C.

We recorded field EPSPs (fEPSPs) from the CA1 stratum radiatum by using an extracellular glass pipette (3–5 MΩ) filled with ACSF. Schaffer collateral/commissural fibers in the stratum radiatum were normally stimulated with a bipolar tungsten electrode placed 200–400 µm away from the recording pipette. Stimulation intensities were chosen to produce an fEPSP with a slope that was 30 to 35% of that obtained with maximal stimulation. LTP was induced electrically by three periods of tetanizations (strong protocol) or one period of tetanization

(weak protocol). Every period of tetanization consisted of 10 trains of 200 Hz stimulation delivered for 200 ms every 5 s at 30 to 35% maximal stimulus intensity.

Drug injection

Bicuculline was obtained from Tocris and was dissolved in 0.9% saline at a final concentration of 0.5 ng/μl. Potassium chloride was obtained from Wako and was dissolved in 0.9% saline at a final concentration of 30 mM. Nocodazole was obtained from Sigma and dissolved in 5% hydroxypropyl β-cyclodextrin (wt/vol) at a final concentration of 10 nM or 100 nM. Clasto-lactacystin-β-lactone (LAC, 32 ng/μl) was obtained from Sigma and dissolved in 2% DMSO. The FGF1 receptor antagonist PD173074 (Selleckchem) was dissolved in DMSO as a stock solution at 500 nM and diluted 1:9 in saline immediately prior to injection. This concentration of PD173074 has been used successfully to block FGFR1 activity (Bansal et al., 2003; Mohammadi et al., 1998). Recombinant FGF1 was purchased from R&D Systems and dissolved in 1X PBS with 0.1% BSA. All experiments using recombinant FGF1 were performed at a load of 25 ng per injection. The compounds were infused (0.5 μl/hemisphere) using a cannula at a rate of 0.1 μl/min. For microinjection, stainless steel guide cannulae (28 gauge; Plastics One) were implanted into the bilateral hippocampus (−2.0 mm AP, ±1.5 mm ML, −1.0 mm DV;(Franklin and Paxinos, 2008). Seven days after surgery, mice were subjected to the experiments. At the end of experimentation, we confirmed the injection sites by injecting 0.5 μl Chicago Sky Blue solution bilaterally, followed by histological analysis of coronal brain slices. Mice that did not receive symmetrical and bilateral injections in the dorsal hippocampus were excluded from the study. The HDAC3 inhibitor T247 was synthesized as reported previously (Suzuki et al., 2013) and dissolved in 1% DMSO at a final concentration of 10 μM. Drug or vehicle was continuously injected bilaterally into the hippocampus using osmotic minipumps (Alzet, model 1002). Minipumps filled with T247 or vehicle were activated on the evening before surgery by incubation in 37°C water to initiate continuous delivery. Bilateral cannulae were inserted into the hippocampus (−2.0 mm AP, ±1.5 mm ML, −1.5 mm DV; (Franklin and Paxinos, 2008). At the end of experiments, all mice were sacrificed, and brain sections prepared to check cannula placement. Anisomycin was purchased from Sigma and dissolved by adding several drops of 1 M HCl. The pH value was adjusted to 7.2 using 1 M NaOH. Anisomycin (150 mg/kg) was injected intraperitoneally 30 min before training.

AAV-mediated gene transfer

AAV-mediated gene transfer was performed as previously reported (Uchida et al., 2010; Uchida et al., 2011b). The expression vectors used for AAV studies were constructed via PCR amplification of the open reading frame of the gene of interest (*Fgf1*, *Crtc1*, *Hdac3*, *Kat5*, *Gfp*, *mCherry*) and the genomic region of promoters (mouse *Camk2a* and human SYN1 promoter). The mutations (*Fgf1res*, *dnCrtc1*, *Crtc1-2SA*, *Crtc1res*, *Crtc1cyt*, *Hdac3res*, *Hdac3-K25A*, *Kat5res*) were made using a KOD Plus Mutagenesis kit (TOYOBO). The primer sequences used for cloning and mutagenesis are shown in Table S1. Recombinant viruses (AAV serotype 2, 8, and 9) were generated by Vector Biolabs. The pAAV-cis plasmids encoding shRNA specific to *Fgf1* (GAAGAAAACCATTATAACACT), *Crtc1* (CGAACAATCCGCGGAAATTTA), *Hdac3* (GCTACTATTGTCTCAATGTGC), or *Kat5* (CGGAGTATGACTGCAAAGGTT) were generated and packaged into AAV8 or AAV9 vector by Vector Biolabs. For virus injections, mice were anesthetized using Avertin (250 mg/kg body weight) and placed in a stereotaxic frame (Kopf). The skull was exposed, and a small portion of the skull above the hippocampus removed bilaterally using a dental drill. Subsequently, the AAV vector was dissolved in physiological saline (0.2 μl) and injected bilaterally into the CA1 (−2.0 mm AP, ±1.5 mm ML, −1.5 mm DV; (Franklin and Paxinos, 2008) or CA3 (−2.0 mm AP, ±2.3 mm ML, −2.3 mm DV) at 0.1 μl/min. The needle was slowly withdrawn after 2 min. To overexpress the gene of interest in the CA subregion (CA1−CA3), the AAV vector was dissolved in physiological saline (0.5 μl) and injected bilaterally into the CA1 (−2.0 mm AP, ±1.5 mm ML, −1.5 mm DV; (Franklin and Paxinos, 2008) at 0.2 μl/min. The needle was slowly withdrawn after 5 min. The mice were allowed to recover for at least three weeks after surgery. Successful transduction of GFP in the hippocampal region was confirmed histologically by immunolabeling.

Immunoprecipitation

Immunoprecipitation was performed as described previously (Uchida et al., 2011b) with minor modifications. The dissected tissues from the CA subregion of 3–4 mice per treatment group were pooled for each

immunoprecipitation experiment and six pooled samples per treatment group were examined in this study. The lysates (1 mg of protein) were pre-cleared using Protein G Plus Agarose beads (Thermo Scientific) for 1 h at 4°C and then incubated for 16 h at 4°C in 5 µg of anti-CRTC1 or normal rabbit IgG (Santa Cruz Biotechnology), followed by incubation for 4 h at 4°C in Protein G Plus Agarose beads. The beads were washed five times with RIPA buffer and the proteins eluted using sample buffer containing 1% SDS. Western blot analyses of the immunoprecipitated anti-CRTC1 samples, normal rabbit IgG samples, and the input samples reserved from the pre-cleared step were performed using anti-CRTC1, anti-CREB, anti-pCREB, or anti-β-actin antibody. A HRP-conjugated anti-mouse IgG antibody (Cell Signaling) or mouse anti-rabbit IgG conformation-specific antibody (Cell Signaling) was used as the secondary antibody. All buffers included 10 mM NaF. Densitometric analysis was performed using ImageQuant software after scanning (Typhoon, GE Healthcare). The primary antibodies are described in Table S2.

Chromatin immunoprecipitation (ChIP) assay

ChIP assay was performed using the SimpleChIP Enzymatic Chromatin IP kit with magnetic beads according to the manufacturer's protocol (Cell Signaling) with minor modifications. Dissected hippocampal tissues (CA subregion) were minced into 1 mm pieces that were immediately frozen on dry ice and stored at −80°C until further use. The pooled dissected samples from 3–4 mice were used as one ChIP sample and a total of 6–11 ChIP samples per experimental group were analyzed. To crosslink the protein-DNA complexes, tissues were placed in 1% formaldehyde for 15 min at room temperature. Fixation was quenched by adding glycine at a final concentration of 0.125 M. The tissues were washed three times with ice-cold PBS containing protease inhibitors (Complete Tab, Roche Diagnostics). The purified nuclear samples were treated with Micrococcal Nuclease to digest DNA to an average length of 150–900 bp, sonicated to disrupt the nuclear membrane, and finally incubated overnight at 4°C with the appropriate antibody (Table S2). All assays included normal rabbit IgG (Santa Cruz Biotechnology) and no-antibody immunoprecipitations to control for the specificity of each antibody. Chromatin-antibody complexes were collected with ChIP Grade Protein G Magnetic Beads (Cell Signaling) and sequentially washed with low salt (three times) and high salt (once) buffers for antibodies directed against modified histones. For other antibodies used for ChIP, complexes were washed five times with RIPA buffer. The antibody-bound chromatin was eluted in 1X ChIP elution buffer (Cell Signaling), followed by reverse cross-linking and protease K treatment. DNA was purified with DNA purification spin columns supplied in the kit. The purified DNA samples were subjected to quantitative real-time PCR analyses. The primer sequences used are shown in Table S1. Real-time PCR ChIP data were analyzed using the ΔΔCt method and normalized to input as described previously (Kumar et al., 2005; Tsankova et al., 2006). The relative ratios of modified histones and target proteins on the genomic regions of interest between experimental groups are indicated in the figures as reported previously (Uchida et al., 2011b).

SUPPLEMENTAL REFERENCES

Bansal, R., Magge, S., and Winkler, S. (2003). Specific inhibitor of FGF receptor signaling: FGF-2-mediated effects on proliferation, differentiation, and MAPK activation are inhibited by PD173074 in oligodendrocyte-lineage cells. J Neurosci Res *74*, 486-493.

Franklin, K., and Paxinos, G. (2008). The Mouse Brain in Stereotaxic Coordinates. Elsevier Academic Press.

Hagihara, H., Toyama, K., Yamasaki, N., and Miyakawa, T. (2009). Dissection of hippocampal dentate gyrus from adult mouse. J Vis Exp.

Kerimoglu, C., Agis-Balboa, R.C., Kranz, A., Stilling, R., Bahari-Javan, S., Benito-Garagorri, E., Halder, R., Burkhardt, S., Stewart, A.F., and Fischer, A. (2013). Histone-methyltransferase MLL2 (KMT2B) is required for memory formation in mice. J Neurosci *33*, 3452-3464.

Kumar, A., Choi, K.H., Renthal, W., Tsankova, N.M., Theobald, D.E., Truong, H.T., Russo, S.J., Laplant, Q., Sasaki, T.S., Whistler, K.N., *et al.* (2005). Chromatin remodeling is a key mechanism underlying cocaine-induced plasticity in striatum. Neuron *48*, 303-314.

McQuown, S.C., Barrett, R.M., Matheos, D.P., Post, R.J., Rogge, G.A., Alenghat, T., Mullican, S.E., Jones, S., Rusche, J.R., Lazar, M.A., *et al.* (2011). HDAC3 is a critical negative regulator of long-term memory formation. J Neurosci *31*, 764-774.

Milnerwood, A.J., Gladding, C.M., Pouladi, M.A., Kaufman, A.M., Hines, R.M., Boyd, J.D., Ko, R.W., Vasuta, O.C., Graham, R.K., Hayden, M.R., *et al.* (2010). Early increase in extrasynaptic NMDA receptor signaling and expression contributes to phenotype onset in Huntington's disease mice. Neuron *65*, 178-190.

Mohammadi, M., Froum, S., Hamby, J.M., Schroeder, M.C., Panek, R.L., Lu, G.H., Eliseenkova, A.V., Green, D., Schlessinger, J., and Hubbard, S.R. (1998). Crystal structure of an angiogenesis inhibitor bound to the FGF receptor tyrosine kinase domain. EMBO J *17*, 5896-5904.
Pacchioni, A.M., Vallone, J., Worley, P.F., and Kalivas, P.W. (2009). Neuronal pentraxins modulate cocaine-induced neuroadaptations. J Pharmacol Exp Ther *328*, 183-192.
Schaeren-Wiemers, N., and Gerfin-Moser, A. (1993). A single protocol to detect transcripts of various types and expression levels in neural tissue and cultured cells: in situ hybridization using digoxigenin-labelled cRNA probes. Histochemistry *100*, 431-440.
Shumyatsky, G.P., Malleret, G., Shin, R.M., Takizawa, S., Tully, K., Tsvetkov, E., Zakharenko, S.S., Joseph, J., Vronskaya, S., Yin, D., *et al.* (2005). stathmin, a gene enriched in the amygdala, controls both learned and innate fear. Cell *123*, 697-709.
Suzuki, T., Kasuya, Y., Itoh, Y., Ota, Y., Zhan, P., Asamitsu, K., Nakagawa, H., Okamoto, T., and Miyata, N. (2013). Identification of highly selective and potent histone deacetylase 3 inhibitors using click chemistry-based combinatorial fragment assembly. PLoS One *8*, e68669.
Tsankova, N.M., Berton, O., Renthal, W., Kumar, A., Neve, R.L., and Nestler, E.J. (2006). Sustained hippocampal chromatin regulation in a mouse model of depression and antidepressant action. Nat Neurosci *9*, 519-525.
Uchida, S., Hara, K., Kobayashi, A., Fujimoto, M., Otsuki, K., Yamagata, H., Hobara, T., Abe, N., Higuchi, F., Shibata, T., *et al.* (2011a). Impaired hippocampal spinogenesis and neurogenesis and altered affective behavior in mice lacking heat shock factor 1. Proc Natl Acad Sci U S A *108*, 1681-1686.
Uchida, S., Hara, K., Kobayashi, A., Funato, H., Hobara, T., Otsuki, K., Yamagata, H., McEwen, B.S., and Watanabe, Y. (2010). Early life stress enhances behavioral vulnerability to stress through the activation of REST4-mediated gene transcription in the medial prefrontal cortex of rodents. J Neurosci *30*, 15007-15018.
Uchida, S., Hara, K., Kobayashi, A., Otsuki, K., Yamagata, H., Hobara, T., Suzuki, T., Miyata, N., and Watanabe, Y. (2011b). Epigenetic status of Gdnf in the ventral striatum determines susceptibility and adaptation to daily stressful events. Neuron *69*, 359-372.
Vogel-Ciernia, A., Matheos, D.P., Barrett, R.M., Kramar, E.A., Azzawi, S., Chen, Y., Magnan, C.N., Zeller, M., Sylvain, A., Haettig, J., *et al.* (2013). The neuron-specific chromatin regulatory subunit BAF53b is necessary for synaptic plasticity and memory. Nat Neurosci *16*, 552-561.